



Pressure drop characteristics of gas–liquid two-phase flow in vertical miniature triangular channels

T.S. Zhao *, Q.C. Bi

Department of Mechanical Engineering, The Hong Kong University of Science and Technology, Clear Water Bay, Kowloon, Hong Kong, People's Republic of China

Received 26 July 2000

Abstract

Experimental data are presented for the gas velocity, the void fraction, and the pressure drop of upward co-current air–water two-phase flow through vertical miniature triangular channels having hydraulic diameters of 0.866, 1.443 and 2.886 mm, with superficial air velocity ranging from $j_g = 0.1$ to 100 m/s and superficial water velocity ranging from $j_l = 0.08$ to 6 m/s. A correlation is developed for predicting the pressure drops of single-phase laminar and turbulent flow through the miniature triangular channels based on that proposed by Churchill (S.W. Churchill, Friction-factor equation spans all fluid flow regimes, Chem. Eng. 84(24) (1977) 91–92) for circular tubes. This work shows that the pressure drop of two-phase flow in the miniature triangular channels can be well predicted by the Lockhart–Martinelli correlation (R.W. Lockhart, R.C. Martinelli, Proposed correlation of data for isothermal two-phase two-component flow in pipes, Chem. Eng. Prog. 45 (1949) 39–48) if the newly proposed friction factor correlation for single-phase flow is adopted. © 2001 Elsevier Science Ltd. All rights reserved.

Keywords: Air–water two-phase flow; Drift velocity; Void fraction; Frictional pressure drop; Vertical miniature triangular channel

1. Introduction

Gas–liquid two-phase flow is of importance in a wide range of technical applications. Examples include heat transfer systems, distillation processes, steam generators, and numerous chemical industrial processes such as continuous loop reactors, bubble column reactors, gas–liquid pipeline systems and so on. In this work, we are concerned with gas–liquid flows through miniature triangular channels having hydraulic diameters of the order of 1.0 mm. Two-phase flow through such miniature non-circular channels may be encountered in closely arranged catalytic rods or monolithic reactors for fine chemicals industries. As compared with two-phase flow in large round tubes, which have been extensively studied for several decades, two-phase flows through small/mini non-circular channels may exhibit different behaviors due to the fact that surface tension becomes sig-

nificant in small-sized channels with sharp corners. For example, Bi and Zhao [2] visually studied the elongated bubble (Taylor bubble) behaviors in vertical miniature circular and non-circular (triangular and rectangular) tubes filled with stagnant liquid, while for large round tubes, gas bubbles (sphere or ellipsoid in shape) rose up periodically in the tube. As the diameter of the circular tubes became smaller, the upward motion of the gas bubbles was slowed down, and ceased completely when the tube size was sufficiently reduced ($d < 2.9$ mm). However, for the non-circular tubes, the elongated bubble always rose upward even though the hydraulic diameter was as small as 0.866 mm. More recently, Zhao and Bi [3] experimentally investigated the flow of co-current upward air–water two-phase flow in vertical miniature triangular channels. Their experimental results show that, when the channel size was reduced to 0.866 mm in hydraulic diameter, the dispersed bubbly flow pattern, characterized by randomly dispersed bubbles in a continuous liquid phase, was never found, although the other typical flow patterns remained in the channel. Moreover, they identified a so-called capillary

* Corresponding author.

E-mail address: metzhao@ust.hk (T.S. Zhao).

Nomenclature	
C	coefficient in Eqs. (25) and (26)
C_0	distribution parameter
C_l	geometry factor of laminar flow
C_t	geometry factor of turbulent flow
G	fluid mass velocity, $\text{kg s}^{-1} \text{m}^{-2}$
d	tube diameter, m
d_h	hydraulic diameter, m
f	friction factor
f_D	Darcy friction factor
f_F	Fanning friction factor
g	gravitational acceleration, $\text{m}^2 \text{s}^{-1}$
Δh	elevation difference of the two pressure taps, m
j	mixture volumetric flux, m s^{-1}
j_l, j_g	superficial velocities, m s^{-1}
L	length of the channel between the two pressure taps, m
Δp_A	acceleration pressure drop, N m^{-2}
Δp_c	manometer offset due to the altitude difference of the two pressure taps, N m^{-2}
Δp_f	single-phase pressure drop, N m^{-2}
Δp_G	gravitational pressure drop, N m^{-2}
Δp_m	pressure difference readings from the differential pressure transducer, N m^{-2}
Δp_{lo}	frictional pressure drop if liquid only flowed through the channel at the same total mass flow rate, N m^{-2}
Δp_{TP}	pressure drops of two-phase flow, N m^{-2}
Re	Reynolds number defined by tube diameter
Re_{dh}	Reynolds number defined by hydraulic diameter
V_b	drift velocity, m s^{-1}
x	mass quality
X^2	Martinelli parameter defined by Eq. (24)
<i>Subscripts</i>	
g	quantities of gas
i	quantities at inlet of the channel
l	quantities of liquid
o	quantities at outlet of the channel
<i>Greek symbols</i>	
α	void fraction
β	volumetric quality
ϵ	roughness of the inner tube wall, m
ρ	fluid density, kg m^{-3}
ρ_c	average density of water through the connecting tube, kg m^{-3}
Φ_{lo}^2	two-phase frictional multiplier

bubbly flow pattern in the micro-triangular channels, which is characterized by a single train of bubbles, essentially elliptical in shape, spanning almost the entire cross-section of the channel.

Attention in the present work was focused on the study of the pressure drop characteristics of both single-phase and two-phase flow through miniature triangular channels. Single-phase flow through miniature circular and rectangular channels has recently been studied extensively. However, considerable differences exist among different investigators on the effect of channel size on frictional loss in miniature channels. For example, Fukano et al. [4], Mishima and Hibiki [5], and Ide et al. [6] reported that the single-phase frictional loss in a circular tube having a diameter as small as 0.5 mm could be predicted well by the correlations of both laminar and turbulent flows through the conventionally sized channels. However, Yu et al. [7] found that the friction factors in circular tubes with diameters of 19, 52 and 102 μm were slightly lower than the Moody chart values for both laminar flow and turbulent flow. Peng et al. [8] found that the turbulent flow resistance in small rectangular channels having hydraulic diameters of 0.133–0.367 mm was usually smaller than that predicted by the classical channel flow theory, and the Reynolds number for flow transition to fully developed turbulent flow in these microchannels

became much smaller than in large-sized channels. Heun [9] investigated the pressure drops of micro-channel condensers consisting of multiport channels having circular, square, triangular, and “H”-shaped cross-sections. He found that Churchill’s equation [1] could predict the frictional losses of single-phase flow through all the channels when suitable effective diameters were used.

Relatively few papers have reported on the study of frictional losses of single-phase flow through triangular channels. It is to be expected that flow characteristics in a triangular channel become more complicated than those in a circular tube even under the single-phase condition. For example, it has been reported that a secondary flow existed in the channel due to the corner effect [10–12].

The study of two-phase flow through triangular channels is much more scarce in the literature, although a large number of investigations have been reported on the characteristics of two-phase flow through other non-circular channels. Sadatomi et al. [13] experimentally investigated air–water two-phase flow through several vertical non-circular channels including an isosceles triangular duct with apex angle of 20° and height of 55 mm. The frictional pressure drops, the rising velocity of large gas bubbles, and the mean void fraction were reported. Heun [9] studied condensation in flat, multiport channels, one of which was triangular in shape and

had a hydraulic diameter of 0.944 mm. Refrigerant R-134a flowing through the tube was cooled by air flowing across the outside of the tube. Triplett et al. [14] recently reported an experimental investigation of the frictional losses of air–water two-phase flow through horizontal microchannels having semi-triangular cross-sections (triangular with one corner smoothed) with hydraulic diameters of 1.09 and 1.49 mm. They found that the two-phase friction factor based on the homogeneous mixture assumption provided the best agreement with the experimental data for bubbly and slug flow patterns, but the homogeneous mixture model and other widely used correlations over-predicted the frictional pressure drops for annular flow. Most recently, Wölk et al. [15] performed experiments for upward, vertical, two-phase air–water flow through a circular and four different non-circular channels, one of which had an equilateral triangular cross-section, with a side length of 10.43 mm (or 6.1 mm hydraulic diameter). In addition to the observation of flow patterns, they also determined the distribution parameter $C_0 = 1.39 - 0.35\sqrt{\rho_g/\rho_l}$ and drift velocity $V_b = 0.35\sqrt{\Delta\rho g d_h/\rho_l}$ for slug flow in the equilateral triangular channel.

As we know, no data have been published for the study of pressure drop of gas–liquid two-phase flow in triangular channels having a hydraulic diameter on the order of 1.0 mm. We shall report our experimental data for the gas velocity, the void fraction, and the pressure drop of upward, co-current, air–water two-phase flow in vertical, miniature, triangular channels having hydraulic diameters of 0.866, 1.443 and 2.886 mm. Correlations for predicting the pressure drops of both single and two-phase flow through miniature triangular channels will be presented and discussed.

2. Experimental

2.1. Experimental setup

The experiments of upward, co-current, air–water two-phase flow through vertical, miniature, triangular channels were carried out in the test loop schematically shown in Fig. 1. The water was driven by a pump and was regulated by a bypass and valves, while the air was supplied by the laboratory air system. After passing the measuring systems separately, the water and air were routed into the inlet plenum of the test section. In order to enhance the mixing of air and water before entering the test section, the inlet plenum was packed with fine plastic meshes. After passing through the test section, the air–water mixture flowed into a collecting tank from the outlet plenum. The air was then separated and released into the atmosphere and the liquid was drained into the circulating water tank.

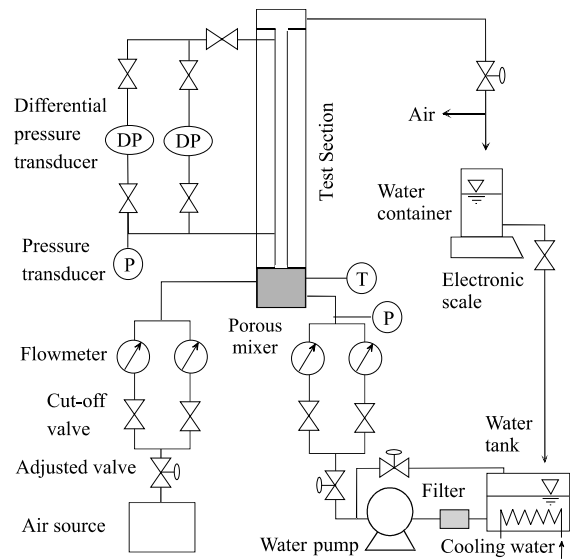


Fig. 1. Schematic of the test facility.

Three equilateral triangular channels (270 mm in length) with side lengths of 5.0, 2.5 and 1.5 mm (corresponding to 2.886, 1.443 and 0.866 mm hydraulic diameter) were tested. The schematic diagram of the test sections is shown in Fig. 2. For the purpose of flow visualization, the test sections were made of Lucite material.

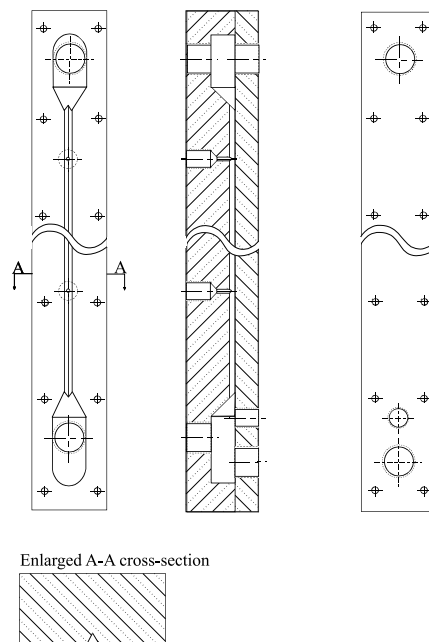


Fig. 2. Geometry diagram of the test section.

For small channels, an accurate measurement of channel size and inner wall roughness is desired for accurately determining flow rates and pressure drops. In this work, a profile projector (Mitutoyo PJ311) was used to measure the sizes of the tested channels, while a surface measuring instrument (Mitutoyo CS-400) was employed to measure the roughness of the inner wall. Pressure drops across the channel were measured by two differential pressure transducers (Rosemont 3051 DP series). The first pressure transducer tap was installed at a distance of 50 mm from the entrance of the channel, while the second tap was located 200 mm away from the first one.

Liquid flow rate through the test section was measured by two turbine-type flow meters (McMillan 101 series) together with one rotameter (Omega FL1405), while the air flow rate was measured by two turbine-type flow meters (McMillan 100 series) and three rotameters (Omega FL1408 and Gilmont GF-5531 series). The pressures at the inlet of the test section and the inlet of the air flowmeters were measured by two pressure transducers (Rosemont 3051 GP series) so that the air flow rate could be corrected based on the ideal gas equation of state.

Analog to digital conversions were carried out by a Keithley Metrabyte DAS-20 A/D board plugged into a Personal Computer, giving 1000 samples per second with 12-bit precision. A specially developed data acquisition software was used to monitor the instant flow rates and pressures such that the experiments could be well controlled. The data were stored in the hard disk of the computer for post-processing of frictional pressure drops.

2.2. Gas velocity measurement

A high-speed motion analyzer (Kodak Ekapro-1000) was employed to visualize bubble behavior in the test sections. The movies of slug bubble motion were recorded at a speed of 3000 pictures per second. Each bubble velocity was measured from consecutive images of the bubble replayed in slow motion (one picture per second) and was calculated based on the time for the bubble to travel a given distance along the test section. The gas velocity was finally calculated by averaging the velocities of three slug bubbles at a given experimental condition.

2.3. Test conditions

The experimental parameters covered in the present work are as follows: for the triangular channel having a side length of 5 and 2.5 mm (corresponding to 2.886 and 1.443 mm hydraulic diameter), the superficial air velocity $j_g = 0.1\text{--}100$ m/s, while the superficial water ve-

locity $j_l = 0.08\text{--}6$ m/s. For the triangular channel having a side length of 1.5 mm (corresponding to 0.866 mm in hydraulic diameter), the superficial air velocity $j_g = 0.1\text{--}100$ m/s, while the superficial water velocity $j_l = 0.1\text{--}3$ m/s. Experiments were carried out under conditions of atmospheric pressure (0.1 MPa) and room temperature of 22°C.

3. Results and discussion

We shall first present the measured gas velocities and compare them with the drift-flux model. We shall then obtain the void fraction based on the measured gas velocities. This will be followed by the presentation of the experimental results of frictional pressure drops of single-phase water flow and air–water two-phase flow through the miniature triangular channels.

3.1. Gas velocity

Fig. 3 presents the measured gas velocities u_g (represented by the open circles) vs. the mixture volumetric flux j for the three tested triangular channels, where $j = (j_l + j_g)$, with j_l and j_g representing the respective superficial velocities of liquid and gas phase. The experimental data were obtained in the slug flow regime. For slug flow in large-sized channels, the liquid bridges usually contain a number of small isolated gas, but for slug flow through miniature triangular channels, Zhao and Bi [3] found that, in most of the cases, almost no isolated gas bubble existed in the liquid bridges between the relatively long gas slugs. This fact suggests that the slug bubble velocity can be regarded as the gas velocity in the slug flow regime. For comparison, Figs. 3(a), (b), and (c) show the drift-flux model given by Wallis [16]

$$u_g = j_g/\alpha = C_0 j + V_b, \quad (1)$$

where α is the void fraction, C_0 the distribution parameter, and V_b is the so-called drift velocity [17]. For slug flow in a large circular tube, it has been shown by Ishii [18] that

$$C_0 = 1.2 - 0.2\sqrt{\rho_g/\rho_l}, \quad (2)$$

$$V_b = 0.35\sqrt{\Delta\rho g d/\rho_l}, \quad (3)$$

where d is the tube diameter, g the gravitational acceleration, and ρ is the fluid density, with the subscripts g and l denoting the quantities of gas and liquid. Similar expressions of C_0 and V_b in a circular tube can also be found from other investigators (e.g., [19]). Eq. (2) implies that the distribution parameter in a circular tube is independent of tube diameter, whereas Eq. (3) suggests

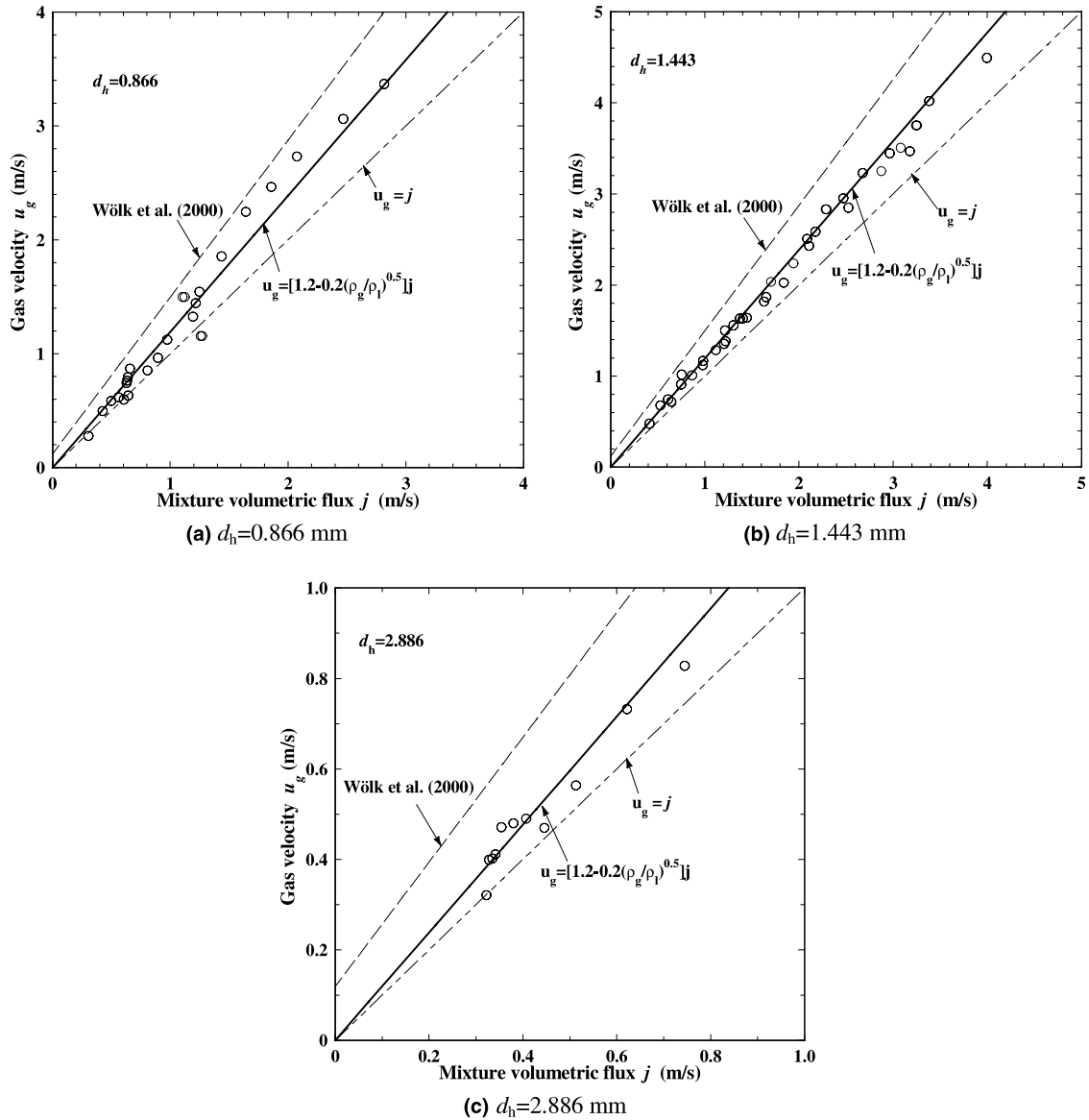


Fig. 3. Gas velocity vs. mixture volumetric flux.

that the drift velocity in a circular tube is proportional to \sqrt{gd} . However, it has also been shown by many investigators [20–22] that, as the tube diameter becomes sufficiently small, the drift velocity diminishes faster than \sqrt{d} and becomes zero when $d < 5$ mm.

Little work has been reported on two-phase flow characteristics for triangular channels in literature. Wölk et al. [15] experimentally investigated the characteristics of upward air–water two-phase flow through a vertical equilateral triangular channel having a hydraulic diameter of $d_h = 6.1$ mm, for which the distribution parameter C_0 and the drift velocity V_b were determined, respectively, as:

$$C_0 = 1.39 - 0.35\sqrt{\rho_g/\rho_l}, \tag{4}$$

$$V_b = 0.35\sqrt{\Delta\rho g d_h/\rho_l}. \tag{5}$$

Apparently, Eqs. (4) and (5) were obtained by extending the distribution parameter C_0 and the drift velocity V_b given by Eqs. (2) and (3) for a large circular tube.

It should be noted that we have previously shown [2] that the drift velocity given by Eq. (3) for a large circular tube cannot be extended to describe the drift velocity in miniature triangular channels ($d_h < 2.886$ mm); the measured drift velocities in the present three miniature

triangular channels having $d_h = 0.866$ and 1.443 mm are only 0.8 and 1.1 mm/s, respectively, which are much smaller than the values predicted by Eq. (5). This is primarily because, in the miniature triangular channels, the surface tension becomes dominant as compared with the buoyancy effect. Since the drift velocities in the present miniature channels are negligibly small, we can therefore ignore them in using the drift-flux model given by Eq. (1). Then, for the distribution parameter given by Eq. (2) and with $V_b \rightarrow 0$, it is seen from Figs. 3(a), (b) and (c) that the drift-flux model with zero drift velocity and $C_0 = 1.2 - 0.2\sqrt{\rho_g/\rho_l}$ is in good agreement with the measured gas velocities for the three

tested miniature channels. We can conclude that, instead of the correlation suggested by Wölk et al. [15], the present measured gas velocities can be well correlated by the drift-flux model with zero drift velocity and $C_0 = 1.2 - 0.2\sqrt{\rho_g/\rho_l}$.

3.2. Void fraction

The void fractions for slug flow in the miniature triangular channels can be obtained from the measured gas velocities based on $u_g = j_g/\alpha$, as indicated in Eq. (1). Fig. 4 presents the void fractions for the tested channels in terms of the volumetric quality defined as

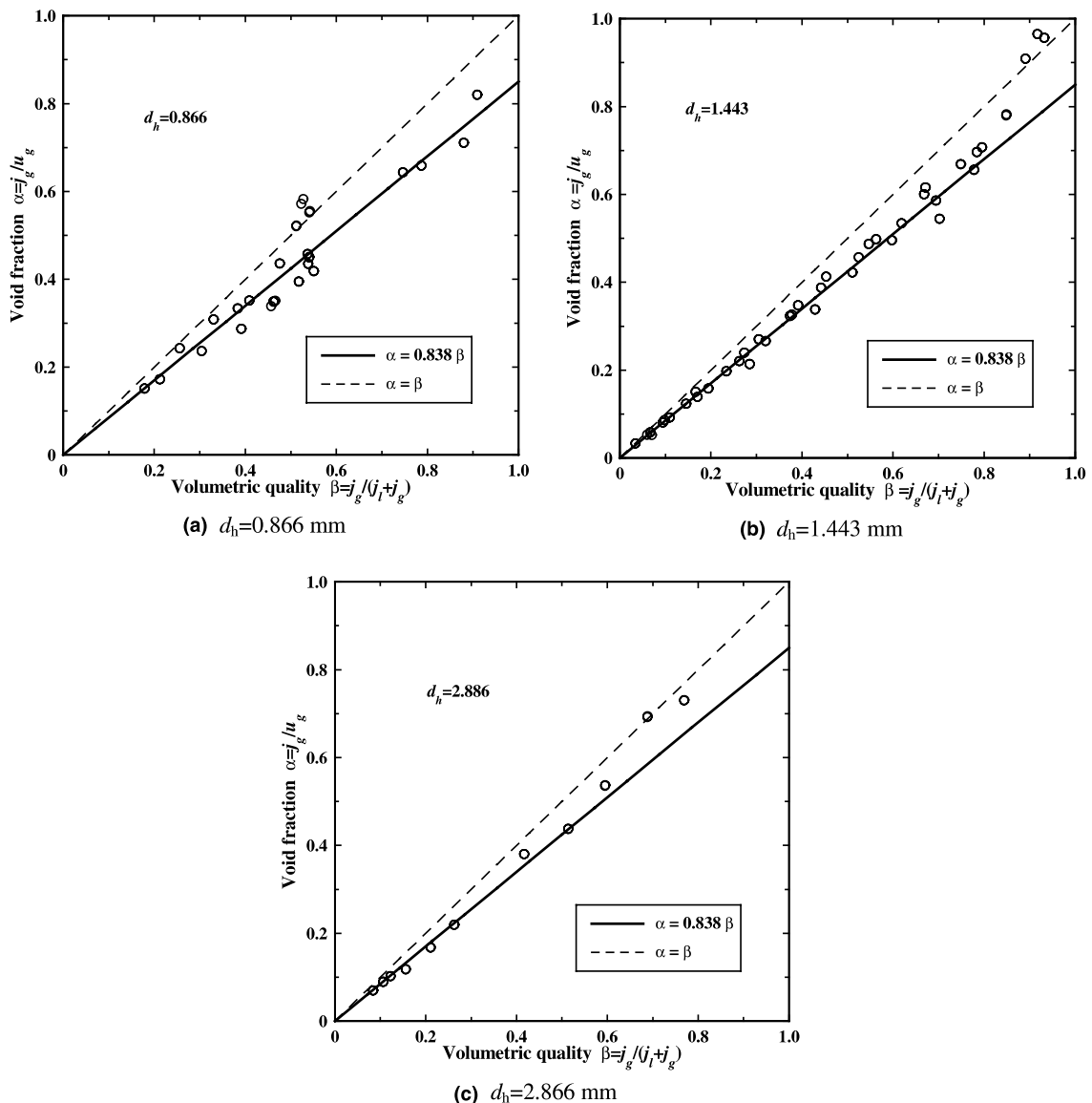


Fig. 4. Void fraction vs. mixture volumetric quality.

$$\beta = j_g/j. \quad (6)$$

Combining Eqs. (1) and (6), and letting $V_b = 0$ leads to

$$\alpha = \frac{1}{C_0} \beta = 0.838\beta. \quad (7)$$

Note that Eq. (7) is very close to $\alpha = 0.833\beta$ for large circular tubes by Armand [23]. Eq. (7) is compared with the experimental data in Fig. 4. It is evident from Fig. 4 that the experimental data for the three tested channels can be best approximated by Eq. (7), 95% of the data falling within the deviation of 10% when $\beta < 0.8$. Eq. (7) will be used to obtain the pressure drop of two-phase flow through the triangular channels.

3.3. Pressure drop

3.3.1. Pressure drop in single-phase flow

The friction factor f considered is defined as usual, i.e.,

$$f = \frac{\Delta p_f}{\rho_1 G^2} \frac{d_h}{L}, \quad (8)$$

where Δp_f represents the measured pressure drops, G is the fluid mass velocity, and L is the length of the channel between the two pressure taps. Note that the friction factor f defined in Eq. (8) is related to the friction factors of Darcy f_D and Fanning f_F , as follows:

$$f = f_F/2 = f_D/8. \quad (9)$$

In this study, we attempt to develop a single equation that is capable of predicting the pressure drops both in single-phase laminar and turbulent flow. This is accomplished based on the following correlation equation proposed by Churchill [1] for a circular tube:

$$f = \left[\left(\frac{C_1}{Re} \right)^{12} + \frac{1}{(A+B)^{3/2}} \right]^{1/12}, \quad (10)$$

where

$$A = \left\{ \frac{1}{\sqrt{C_1}} \ln \left[\frac{1}{(7/Re)^{0.9} + 0.27\epsilon/d} \right] \right\}^{16}, \quad (11)$$

$$B = \left(\frac{37530}{Re} \right)^{16}, \quad (12)$$

with Re representing the Reynolds number defined by the tube diameter and ϵ/d being the relative roughness of the inner tube wall. Eq. (10) is applicable for both the laminar flow regime, reflected by the term C_1/Re and the turbulent regime, reflected by the term $(1/\sqrt{C_1}) \ln[1/((7/Re)^{0.9} + 0.27\epsilon/d)]$, where the constants C_1 and C_t are the so-called geometry factors for laminar and turbulent flow, respectively [13]. For a circular tube, the

friction factors in laminar and turbulent flow regimes are given, respectively, by [1]

$$f_F = \frac{16}{Re} \quad (13)$$

and

$$\frac{1}{\sqrt{f}} = 2.457 \ln \left[\frac{1}{(7/Re)^{0.9} + 0.27\epsilon/d} \right]. \quad (14)$$

An examination of Eqs. (13) and (14), incorporating Eq. (9), leads to $C_1 = C_{10} = 8$ and $C_t = C_{t0} = 1/2.457^2$ for circular tubes. Note that the laminar and turbulent geometry factors for circular tubes are now designated by C_{10} and C_{t0} .

We obtain the geometry factors C_1 and C_t for an equilateral triangular channel such that Eq. (10) can be extended to predict the frictional pressure drops of single-phase flow through a triangular channel. The values of C_1 for various channel cross sections are documented by Kakac et al. [24]. For an equilateral triangular channel, it can be shown that

$$f_F = \frac{13.33}{Re}, \quad (15)$$

which, together with Eq. (9), leads to $C_1 = C_{1\Delta} = 13.33/2 = 6.67$, with $C_{1\Delta}$ denoting the laminar flow geometry factor for an equilateral triangular channel.

It has been shown by Sadatomi et al. [13] that the turbulent flow geometry factor C_t for a triangular or a rectangular channel is closely related to the laminar and the turbulent flow geometry factors C_{10} and C_{t0} for a circular tube by

$$\frac{C_t}{C_{t0}} = \left[0.0154 \frac{C_1}{C_{10}} - 0.012 \right]^{1/3} + 0.85, \quad (16)$$

which was obtained empirically by curve-fitting the experimental data for the friction factors of turbulent flow through channels having rectangular, triangular, and circular cross-sections. Eq. (16) gives the most accurate prediction for Reynolds numbers ranging from 10^4 to 10^5 [13]. Substituting $C_1 = C_{1\Delta} = 6.67$, $C_{10} = 8$, and $C_{t0} = 1/2.457^2$ in Eq. (16) yields the turbulent geometry factor for a triangular channel $C_{t\Delta} = 1/2.529^2$. As a result, the laminar and turbulent geometry factors for a triangular channel are given by

$$C_1 = C_{1\Delta} = 6.67; \quad C_t = C_{t\Delta} = 0.156. \quad (17)$$

We now compare the experimental data with the prediction by Eq. (10) with the geometry factors given by Eq. (17) for pressure drops of single-phase water flow through the three triangular channels in Figs. 5(a), (b) and (c), respectively, in terms of the friction factor f defined by Eq. (8) vs. the Reynolds number Re_{dh} defined based on the hydraulic diameter d_h . It is seen from these figures that Eq. (10) with $C_1 = 6.67$ and $C_t = 0.156$

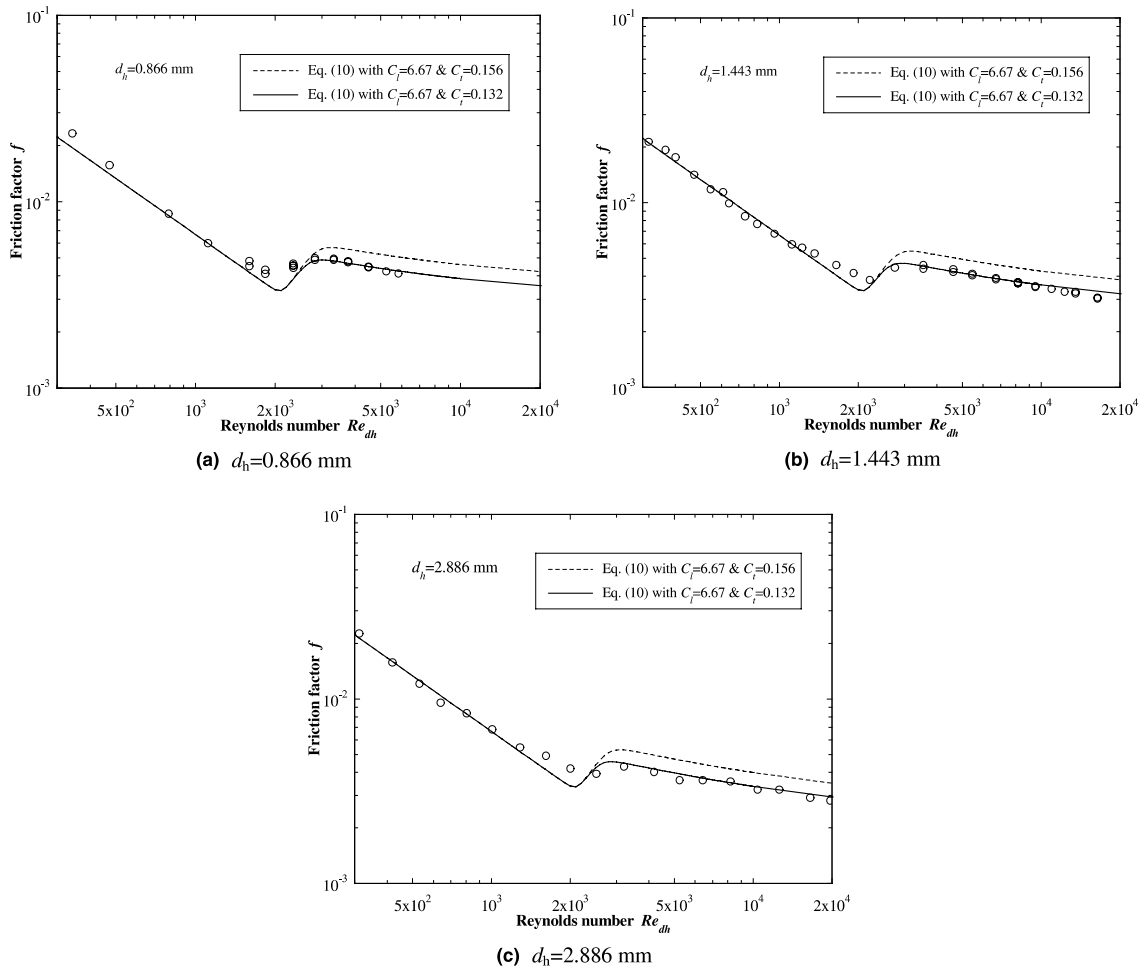


Fig. 5. Frictional factor of single-phase water flow in the miniature triangular channels.

deviates somewhat from the experimental data in the turbulent flow region, but an excellent agreement is observed in the laminar flow region. The reason lies in the fact that the laminar flow geometry factor $C_l = 6.67$ is obtained from the classical channel flow theory, as indicated by Eq. (15), while the turbulent geometry factor $C_t = 0.156$ is obtained from the empirical Eq. (16) for relatively large non-circular channels. Moreover, for a triangular channel, the flow in the corner regions may remain laminar, even though the core flow in the channel is fully turbulent. This phenomenon may become more significant when channel sizes are reduced. To develop a more accurate correlation, a new turbulent flow geometry factor, C_t , reflecting the above-mentioned influences, is needed. This is accomplished by curve-fitting the experimental data. Eq. (10) can best fit the experimental data for the three tested miniature triangular channels with

$$C_l = C_{l\Delta} = 6.67; \quad C_t = C_{t\Delta} = 0.132. \quad (18)$$

The laminar flow geometry factor C_l in Eq. (18) remains the same as in Eq. (17). As evident from Figs. 5(a)–(c), Eq. (10) with the geometry factors given by Eq. (18), designated the solid curve, is in good agreement with the data for all the channels.

3.3.2. Pressure drop in two-phase flow

The data reduction of the pressure drops of two-phase flow through the triangular channels, Δp_{TP} , was carried out by the following balance equation:

$$\Delta p_{TP} = \Delta p_m + \Delta p_c - \Delta p_G - \Delta p_A, \quad (19)$$

where Δp_m represents the pressure difference readings from the differential pressure transducer, Δp_c is the manometer offset due to the altitude difference of the two pressure taps, Δp_G the gravitational pressure drop, and Δp_A is acceleration pressure drop. The manometer offset, Δp_c , was obtained from

$$\Delta p_c = \rho_c g \Delta h, \quad (20)$$

where ρ_c is the average density of water through the tube connecting the pressure transducer and the pressure taps and $\Delta h = 0.2$ m is the altitude difference. In this work, the average density of water ρ_c was determined at the room temperature of 22°C and $\Delta h = 0.2$ m. Δp_G and Δp_A were obtained, respectively, from

$$\Delta p_G = \frac{g\Delta h}{2} \{ [\alpha\rho_g + (1 - \alpha)\rho_1]_o + [\alpha\rho_g + (1 - \alpha)\rho_1]_i \} \quad (21)$$

and

$$\Delta p_A = G^2 \left\{ \left[\frac{x^2}{\alpha\rho_g} + \frac{(1-x)^2}{(1-\alpha)\rho_1} \right]_o - \left[\frac{x^2}{\alpha\rho_g} + \frac{(1-x)^2}{(1-\alpha)\rho_1} \right]_i \right\}, \quad (22)$$

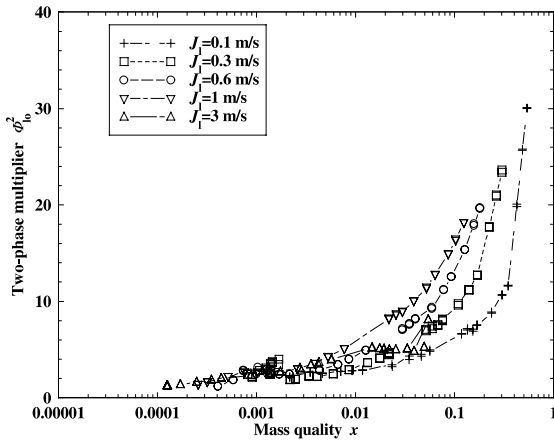
where the void fraction $\alpha = 0.838\beta$ was used in this work, with β being the volumetric quality.

To predict the frictional pressure drops of two-phase flow through miniature triangular channels, Lockhart–Martinelli’s method [25] is used in this study. We now accordingly introduce the two-phase multipliers as follows:

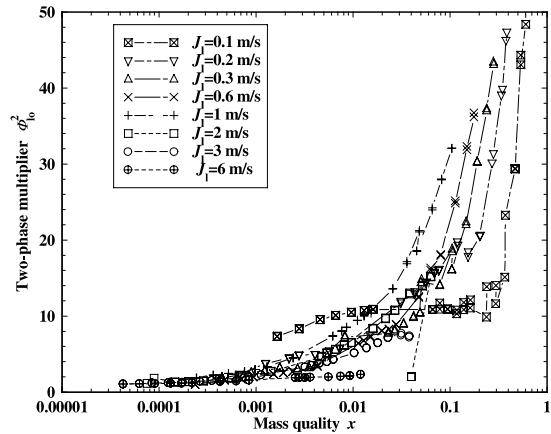
$$\Phi_l^2 = \frac{\Delta p_{TP}}{\Delta p_l}, \quad \Phi_{lo}^2 = \frac{\Delta p_{TP}}{\Delta p_{lo}}, \quad \Phi_g^2 = \frac{\Delta p_{TP}}{\Delta p_g}, \quad (23)$$

where Δp_l and Δp_g represent, respectively, the frictional pressure drop that would result if the liquid or the gas flowed alone through the channel, while Δp_{lo} denotes the frictional pressure drop that would result if liquid only flowed through the channel at the same total mass flow rate. Note that the pressure drops Δp_l , Δp_g , and Δp_{lo} can be obtained from Eqs. (8) and (10), as presented in the previous section.

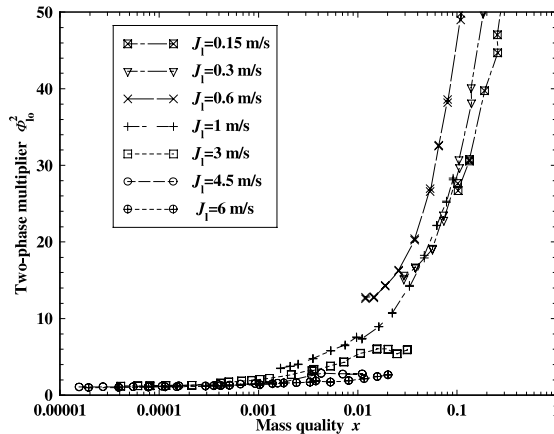
The variations of the two-phase multiplier Φ_{lo}^2 with the thermodynamic quality x for various liquid flow rates through the triangular channels of $d_h = 0.866, 1.443$ and



(a) $d_h = 0.866$ mm



(b) $d_h = 1.443$ mm



(c) $d_h = 2.886$ mm

Fig. 6. Two-phase frictional multiplier Φ_{lo}^2 vs. mass quality x .

2.886 mm are presented in Fig. 6. It is seen from Figs. 6(a), (b) and (c) that the curve of $\Phi_{l_0}^2$ shifts left with the increase of the liquid superficial velocity j_l , implying that, at the same quality, a higher liquid superficial velocity results in a higher pressure drop. It is interesting to note from Fig. 6(a) that the measured two-phase multiplier $\Phi_{l_0}^2$ exhibits an abrupt change at a mass quality of about 0.002. This fact may suggest that the transition of flow pattern from capillary bubble flow to slug flow takes place under this particular condition. Similar behavior was also observed by Wambsganss et al. [26] for air–water two-phase flow through a horizontal rectangular channel having a hydraulic diameter of 5.44 mm. The reason why other flow pattern transitions are not noticeable from Fig. 6 may be attributed to the fact that their transitions are too gradual to be seen from the measured pressure drops.

The two-phase flow multipliers Φ_l^2 and Φ_g^2 are often correlated in terms of the Martinelli parameter X^2 defined as

$$X^2 = \frac{(\Delta p)_l}{(\Delta p)_g} \quad (24)$$

The original correlation was given in a graphical form by Lockhart and Martinelli [25]. Later, Chisholm [27] correlated the multipliers Φ_l^2 and Φ_g^2 with the parameter X^2 in the form as follows:

$$\Phi_g^2 = 1 + CX + X^2 \quad (25)$$

and

$$\Phi_l^2 = 1 + \frac{C}{X} + \frac{1}{X^2}, \quad (26)$$

where the coefficient C is a dimensionless parameter whose value depends on whether the liquid and gas are

Table 1
Empirical constants curves suggested by Chisholm [27]

Liquid	Gas	Subscript	C
Turbulent	Turbulent	tt	20
Laminar	Turbulent	lt	12
Turbulent	Laminar	tl	10
Laminar	Laminar	ll	5

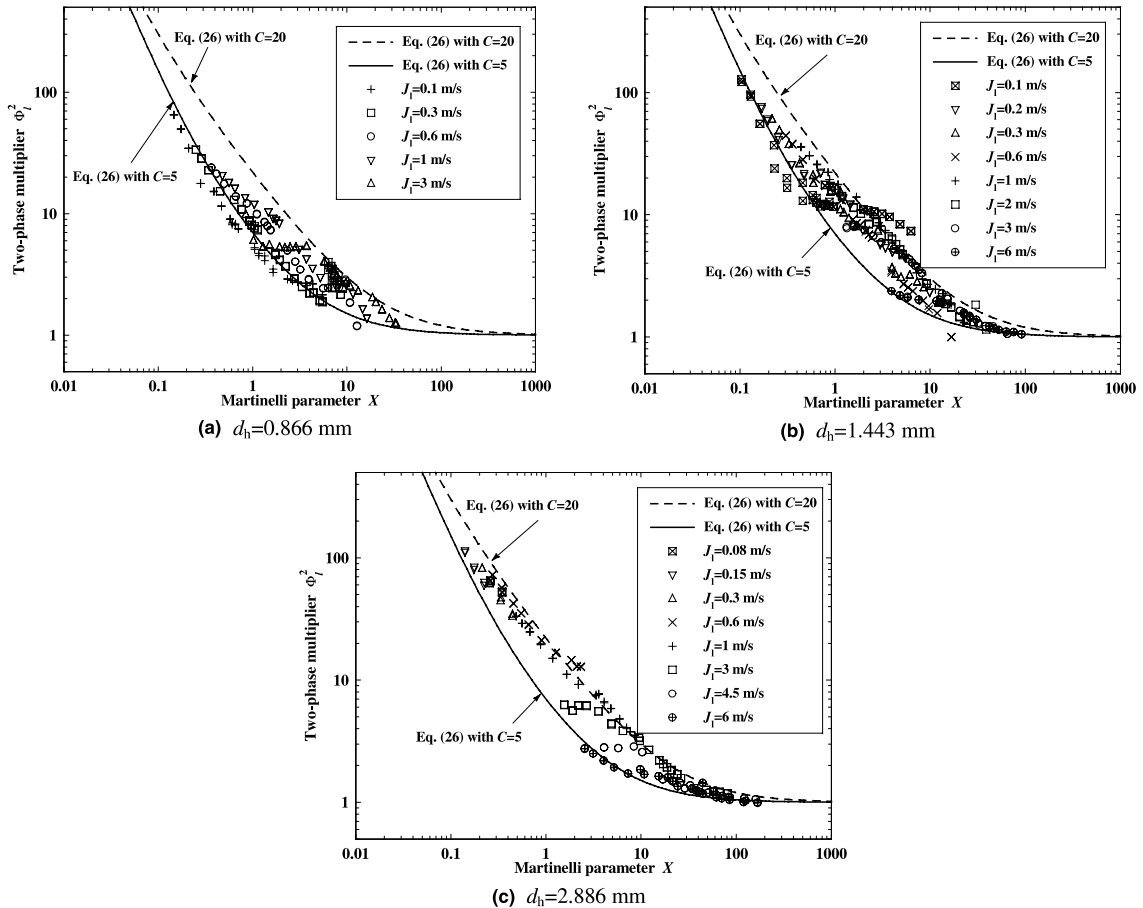


Fig. 7. Two-phase frictional multiplier Φ_l^2 vs. Martinelli parameter X .

laminar or turbulent. The values of C suggested by Chisholm [27] are listed in Table 1.

The variations of the measured two-phase frictional multiplier Φ_{lo}^2 with the Martinelli parameter x for the three miniature triangular channels of $d_h = 0.866, 1.443$ and 2.886 mm are displayed, respectively, in Figs. 7(a), (b) and (c). Shown also in Fig. 7 are the curves predicted by Eq. (26) for $C = 5$ and $C = 20$. It is evident from Fig. 7 that the experimental data are reasonably predicted by the Lockhart–Martinelli correlation, reflected by the fact that all the data largely fall between the curves for $C = 5$ and $C = 20$, except the case at very low superficial liquid velocities.

4. Conclusions

Experimental data for gas velocity, void fraction, and pressure drop of upward co-current air–water two-phase flow in vertical miniature triangular channels have been reported in this paper.

As shown, the measured gas velocity can be well correlated by the drift-flux model with assumed zero drift velocity and the distribution parameter $C_0 = 1.2 - 0.2\sqrt{\rho_g/\rho_l}$. A correlation of the void fraction in terms of the volumetric quality has been obtained. A correlation equation is developed for predicting the frictional pressure drops of single-phase laminar and turbulent flow in miniature triangular channels based on that proposed by Churchill [1] for circular tubes. This correlation is shown to be in good agreement with the measured pressure drop of single-phase water flow through the three tested miniature channels. Finally, it has been shown that two-phase frictional pressure drops can be well predicted by the Lockhart–Martinelli correlation if the newly proposed friction factor correlation for single-phase flow is adopted.

Acknowledgements

This work was supported by Hong Kong RGC Earmarked Research Grants No. HKUST 6045/97E. The first author gratefully acknowledges the Visiting Scholar Foundation of the State Key Laboratory of Multiphase Flow in Power Engineering at Xi'an Jiaotong University.

References

- [1] S.W. Churchill, Friction-factor equation spans all fluid flow regimes, *Chem. Eng.* 84 (24) (1977) 91–92.
- [2] Q.C. Bi, T.S. Zhao, Taylor bubbles in miniaturized circular and noncircular channels, *Int. J. Multiphase Flow* 27 (3) (2000) 561–570.
- [3] T.S. Zhao, Q.C. Bi, Co-current air–water two-phase flow patterns in vertical triangular microchannels, *Int. J. Multiphase Flow*, 2001, in press.
- [4] T. Fukano, A. Kariyasaki, M. Kagawa, Characteristics of time varying void fraction in isothermal air–water concurrent flow in a horizontal capillary tube, in: *Proceedings of the Third ASME/JSME Thermal Engineering Joint Conference*, ASME, New York, NY, USA, 1991, pp. 127–134.
- [5] K. Mishima, T. Hibiki, Some characteristics of air–water two-phase flow in small diameter vertical tubes, *Int. J. Multiphase Flow* 22 (1996) 703–712.
- [6] H. Ide, H. Matsumura, Y. Tanaka, T. Fukano, Flow patterns and frictional pressure drop in gas–liquid two-phase flow in vertical capillary channels with rectangular cross section, *Trans. JSME Ser. B* 63 (1997) 452–460.
- [7] D. Yu, R. Warrington, R. Barron, T. Ameel, An experimental investigation of fluid flow and heat transfer in microtubes, in: *Proceedings of the ASME/JSME Thermal Engineering Conference 1*, ASME (1995) 523–530.
- [8] X.F. Peng, G.P. Peterson, B.X. Wang, Frictional flow characteristics of water flowing through rectangular microchannels, *Exp. Heat Transfer* 7 (4) (1994) 249–264.
- [9] M.K. Heun, Performance and optimization of microchannel condensers, Ph.D. thesis, University of Illinois at Urbana-Champaign, 1995.
- [10] J. Nikurades, Untersuchungen über turbulente strömung in nicht kreisförmigen rohren, *Ing.-Arch.* 1 (1930) 306–332.
- [11] C.J. Cremers, E.R.G. Eckert, Hot-wire measurements of turbulence correlations in a triangular duct, *ASME J. Appl. Mech. Trans.* 29 (1962) 609–614.
- [12] A.M.M. Aly, A.C. Trupp, A.D. Gerrard, Measurements and prediction of fully developed turbulent flow in an equilateral triangular duct, *J. Fluid Mech.* 85 (part 1) (1978) 57–83.
- [13] Y. Sadatomi, Y. Sato, S. Saruwatari, Two-phase flow in vertical noncircular channels, *Int. J. Multiphase Flow* 8 (1982) 641–655.
- [14] K.A. Triplett, S.M. Ghiaasiaan, S.I. Abdel-Khalik, D.L. Sadowski, Gas–liquid two-phase flow in microchannels, Part II: void fraction and pressure drop, *Int. J. Multiphase Flow* 25 (1999) 395–410.
- [15] G. Wölk, M. Dreyer, H.J. Rath, Flow patterns in small diameter vertical non-circular channels, *Int. J. Multiphase Flow* 26 (2000) 1037–1061.
- [16] G.B. Wallis, *One Dimensional Two-phase Flow*, McGraw-Hill, New York, 1969.
- [17] T.B. Benjamin, Gravity currents and related phenomena, *J. Fluid Mech.* 31 (part 2) (1968) 209–248.
- [18] M. Ishii, One-dimensional drift-flux model and constitutive equations for relative motion between phases in various two-phase flow regimes, ANL Report ANL -77-47, 1977.
- [19] D.J. Nicklin, J.O. Wilkes, J.F. Davidson, Two-phase flow in vertical tubes, *Trans. J. Chem. Eng.* 40 (1962) 61–68.
- [20] E.E. Zukoski, Influence of viscosity, surface tension, and inclination angle on motion of long bubbles in closed tubes, *J. Fluid Mech.* 25 (part 4) (1966) 821–837.

- [21] K.W. Tung, J.Y. Parlange, Note on the motion of long bubbles in closed tube – influence of surface tension, *Acta Mech.* 24 (1976) 313–317.
- [22] Y. Kataoka, H. Suzuki, M. Murase, Drift-flux parameters for upward gas flow in stagnant liquid, *J. Nucl. Sci. Technol.* 24 (1987) 580–586.
- [23] A.A. Armand, The resistance during the movement of a two-phase system in horizontal pipes, *Izv. Vses. Teplotekh. Inst.* 1 (1946) 16–23 (AERE-Lib/Trans 828).
- [24] S. Kakac, R.K. Shah, W. Aung, *Handbook of Single-phase Convective Heat Transfer*, Wiley, New York, 1987.
- [25] R.W. Lockhart, R.C. Martinelli, Proposed correlation of data for isothermal two-phase two-component flow in pipes, *Chem. Eng. Prog.* 45 (1949) 39–48.
- [26] M.W. Wambsganss, J.A. Jendrzeczyk, D.M. France, Determination and characteristics of the transition to two-phase slug flow in small horizontal channels, *J. Fluids Eng.* – Trans. ASME 116 (1994) 140–146.
- [27] D. Chisholm, A theoretical basis for the Lockhart–Martinelli correlation for two-phase flow, *Int. J. Heat Mass Transfer* 10 (1967) 1767–1778.